Ocean loading tides in space techniques and implications for mass centre variations

Hans-Georg Scherneck* Rüdiger Haas * Frank H. Webb §

Abstract

Ocean tide loading in VLBI and GPS is examined at a limited set of stations. We highlight the problem of discriminating the frame motion induced by the time varying component of the centre of mass of the ocean, which is to cause a counterbalancing tide in the mass centre of the solid earth. We find that the frame origin of the GPS system is not susceptable to these tides.

Our route of attack is to use VLBI to assess the quality of the loading model and to compute variants of ocean loading for testing them with GPS.The situation for studying tidal site and frame motion is anticipated to be favorable when precise point position is used in contrast to baseline or network solutions. Using more that one year long time-series of GPS point positions at two hour interval we obtain estimates of tide related parameters at submillimeter precision. This is sufficient for resolving particularly some lunar effects as these are less perturbed by environmental effects than their solar counterparts.

We find further that motion due to ocean loading tides is detected in VLBI in all three spatial components, of which the horizontal results are new.

Introduction

Activities in ocean tide loading at Onsala Space Observatory comprise presently a new model for the IERS and verification/assessment of models using VLBI and GPS. Ocean loading tides are computed from a given ocean tide model using a convolution integral with the point load function as a kernel. The point load function is the Green's function of the deformation problem and is derived from the elastic and density structure of an earth model. For a background refer to Farrell (1972), and Scherneck (1991).

For use as an international standard in space geodesy the IERS endorses an ocean loading model in their Conventions document (McCarthy, 1996). The crustal motion due to ocean loading tides is regularly at the one to ten millimetre level. The maximum displacement at any one of the fundamental stations listed in the ITRF catalogue is found at Fortaleza (Brasil) with 66 mm in the vertical and 15 mm the horizontal (scanned inside an 18.6 yr interval). With an increasing resolving power of the methods and more and more data being available for analysis, the need for more and more accurate ocean loading parameters at more and more stations continues.

As ocean tide matters mature after the conclusion of a number of modelling and observation efforts, the idea behind the suggestion for an update of the standards, IERS Conventions 2000, is to achive a greater level of consistency between different chapters of the standards, and to come up with a model that is internally more consistent at the same time. To get perspective on that issue, the previous loading model is based on Le Provost et al. (1994) tides with augmentation for missing oceanic areas from other models or, as in the case of the Bay of Fundy, without. The Bay of Fundy is an area with extremely large semidiurnal tides, complicated coastlines and therefore difficult to model—in particular in a hydrodynamic model that at the same time attempts to represent the ocean on global scales. This piecemeal situation is somewhat relaxed now with the advent of the CSR3.0 ocean tide of Eanes and Bettadpur (1995). Still, the Bay of Fundy is absent, but the Mediterranean (and Kattegatt) is well represented. Additional virtues are that TOPEX/Poseidon satellite altimetry has been used to assimilate long-wavelength features, and that these have considerably improved the parameters representing the centre of mass of the ocean.

* *Onsala Space Observatory, Chalmers University of Technology, S-439 92 ONSALA, Sweden*
phone +46 31 7725500, fax +46 31 7725590, corresponding author: Scherneck, e-mail: hgs@oso.chalmers.se
§ Jet Propulsion Laboratory, Pasadena, Calif.

In the centre of the scope of this paper is the attempt to discern tide induced motion in space-based determinations of point positions on the solid earth. Earlier work in this respect has been presented by Sovers (1994), observing vertical ocean tide loading effects in VLBI. Haas (1996) and Haas and Schuh (1998) have analyzed and discussed these effects primarily in conjunction with devising an improved observation model for solid earth tides in VLBI (Schuh and Haas, 1998).

Centre of mass tides

At first, ocean loading tides are concieved as a deformation of the earth. The traditional reference point has been the centre of mass of the earth excluding the load itself. Seen from space, the centre of mass of the solid earth (and core) moves in a mirror fashion to the centre of mass of the load in order to preserve the joint centre of mass as fixed.

The centre of mass of the tide is

$$\mathbf{X}_{tide} = \frac{1}{M_{tide}} \int_{\mathcal{O}} \mathbf{x}\, dm$$

where M is the mass of the earth and dm is the tidal mass distribution in the ocean $\mathcal{O}$. It is counterbalanced by the condition

$$M_{Earth}\mathbf{X}_{earth} + M_{tide}\mathbf{X}_{tide} = 0$$

This motion is observable with satellite techniques only, since the physical centre of the orbits is in the joint mass centre. In VLBI, as the technique is tied to nearly infinitely distant quasars, the translational motion of a baseline vector cannot be resolved. Surface geodetic techniques are insensitive to this motion. This is seen in inspecting Love number relations. The differences k'_1 - h'_1, k'_1 - l'_1, and k'_1 - l'_1 are invariant, and k'_1 = -1 is the value of the load Love number for the secondary potential corresponding to a reference origin in the joint mass centre (to first order in perturbations). The combinations apply to e.g. the components tilt $(1 + k' - h')$, gravity $(1 + 2h' - [(n + 1)/n]k')$, vertical deflection $(1 + k' - l')$, areal strain $(2h' - n(n + 1)l')$ with spherical harmonic degree $n = 1$ for this style of motion.

The implication of the joint centre of mass of load and deformed body as the physical centre of the gravitational forces acting on the satellites and thus the fixing of translation of the reference frame might appear strong at first sight. However, when orbital parameters are solved from GPS observations at tracking stations, a number of parameters have to be solved for which independent control does not exist (e.g. clock drift, dissipative forces on the spacecrafts) and a number of modelling conditions are used that influence the orbit solutions. Among others, effects due to ocean tide loading and atmospheric loading are usually neglected. Thus, estimated parameters might be biased at a comparatively high degree by systematic effects. To put it simply: if the cohorent, translational motions of sites in the tracking network is not properly reduced in the orbital analysis, the motion is propagated into the orbital parameters. From there the bias propagates into the site positions estimated at an observer's station. In consequence, the differential motion between tracking stations and user stations is to a great extent (probably 100 percent) unaffected by the bias. The bias will therefore only potentially appear as a problem when different satellite techniques are used together inconsistently.

Data analysis

To test the sensitivity of space techniques to ocean loading effects we have compared predicted ocean tide loading parameters with solutions from VLBI and GPS.

VLBI data

For VLBI the data analysis is described in Haas (1996). The data sets analyzed here come from the archive at Goddard Space Flight Center and comprise about 2000 observing sessions, or 1.6 Mio. individual radio source observations, round 70 percent of the available stock. Since VLBI is a baseline network method, the retrieval of residual tidal motion at one station requires that the remaining stations are modelled. The choice of model will therefore cause a side-effect on the residual of the free station. In the analysis a number interesting stations (typically 10 to 20) are freed (model set to null) and the remaining ones (80 to 90) are fixed to the modelled motion. The estimated parameters consider cotidal

motion (amplitude and phase with respect to the astronomical partial tide). The new ingredient in this study is the extension to include horizontal components in the analysis of the baseline residual of each observation. Only cotidal parameters for M_2 and O_1, i.e. significant lunar tides, were targeted. Haas and Schuh (1998) have been successful to retrieve vertical tidal motion at both lunar, solar, and sidereal frequencies. In this study, however, we excluded the latter terms for the sake of comparison with GPS data.

GPS point positioning data

For GPS, the precise single point positioning method available in the GIPSY/OASIS-II software has been employed (Webb and Zumberge, 1993; Zumberge et al., 1997). We have chosen this processing mode since it does not perform range differencing, and since it is free from the interdependencies of motions and errors at simultatneous observations typically experienced in network solutions. Thus the data is expected to preserve a more complete set of range variations between the satellite and the receiver. Spacecraft positions are taken from JPL orbit solutions which include an accurate clock parameter as a prerequisite to solve single point positions accurately. The huge amount of available observations allows to solve for long, almost uninterrupted time-series at sampling rates suitable for tide analysis.

Positions were estimated with the GIPSY Kalman filter at two hours interval, atmospheric parameter at 5 minutes interval assuming a random walk noise model of the zenith delay. Each sample was taken to represent the mean position of the station at the central time of the two-hour interval. The 3-D series were transformed into a local system with east, north, and vertical axes. Solid earth tide displacements were subtracted as usual in GIPSY. The point-positioning time-series were then analyzed with a standard least-squares tidal analysis program.

Loading models

On the modelling side different sets of loading coefficients were computed from three global ocean tide models, NSWC - Schwiderski and Szeto (1982), Grenoble - Le Provost et al. (1994), and CSR3.0 - Eanes and Bettadpur (1995). For details concerning the computation see Scherneck, (1991). These computations are identical (and some variants) from those available from the IERS standards (McCarthy, 1996). For the GPS analysis alternate options to include or not include the centre of mass tide were applied (Scherneck and Webb, 1998).

We have used various methods and options to model and discriminate atmospheric loading, but the results are hitherto too unsystematic and weak for coming into the focus of the discussion.

Discussion

In GPS we generally find very large perturbations at solar and sidereal cycles. The origin of the solar cycles (24/n hours period) is most probably found in the reinitiation of the Kalman filter each midnight. The sidereal period and its upper harmonics, however, might have a less clear origin, one candidate being satellite orbit errors (range effective features that are fixed in the orbital frame will cause near sidereal (sub-) periods seen from an earth-fixed point). We therefore limit the discussion to lunar species in both techniques.

Ocean loading models appear to generally explain a greater amount of the tidal residuals at the lunar frequencies. This is particularly true of VLBI where even most of the horizontal motion can be explained by ocean loading tides. Results for the stations of this survey are compiled in Table 1. A general finding is that the models leave residuals in all components that are significant as compared to the confidence limit of the observations. Reasons may be threefold: There are possible errors in the ocean tide, biases in the VLBI analysis due to the loading model at the fixed stations, and biases due to the solid earth tide model. The discrepancies, however, are larger than what could be explained by loading effects as propagated through different earth rheologies. Take Wettzell as an example. The continental structure of central Europe departs only slightly from the continental PREM model (Dziewonski and Anderson, 1981), which was used to compute the loading Green's function. Yet at this station the weakest reduction of tide motion is found. Of course, the unexplained motion could arise due to various combinations of the problems pointed out, being different at each site.

As an example we show a phasor diagram for Westford, Massachusetts (Fig. 1) where we include different models and variants. The CSR3.0 model has been used in the VLBI analysis at the other stations. We find a good agreement with the Schwiderski model (Schwiderski and Szeto, 1982) and in

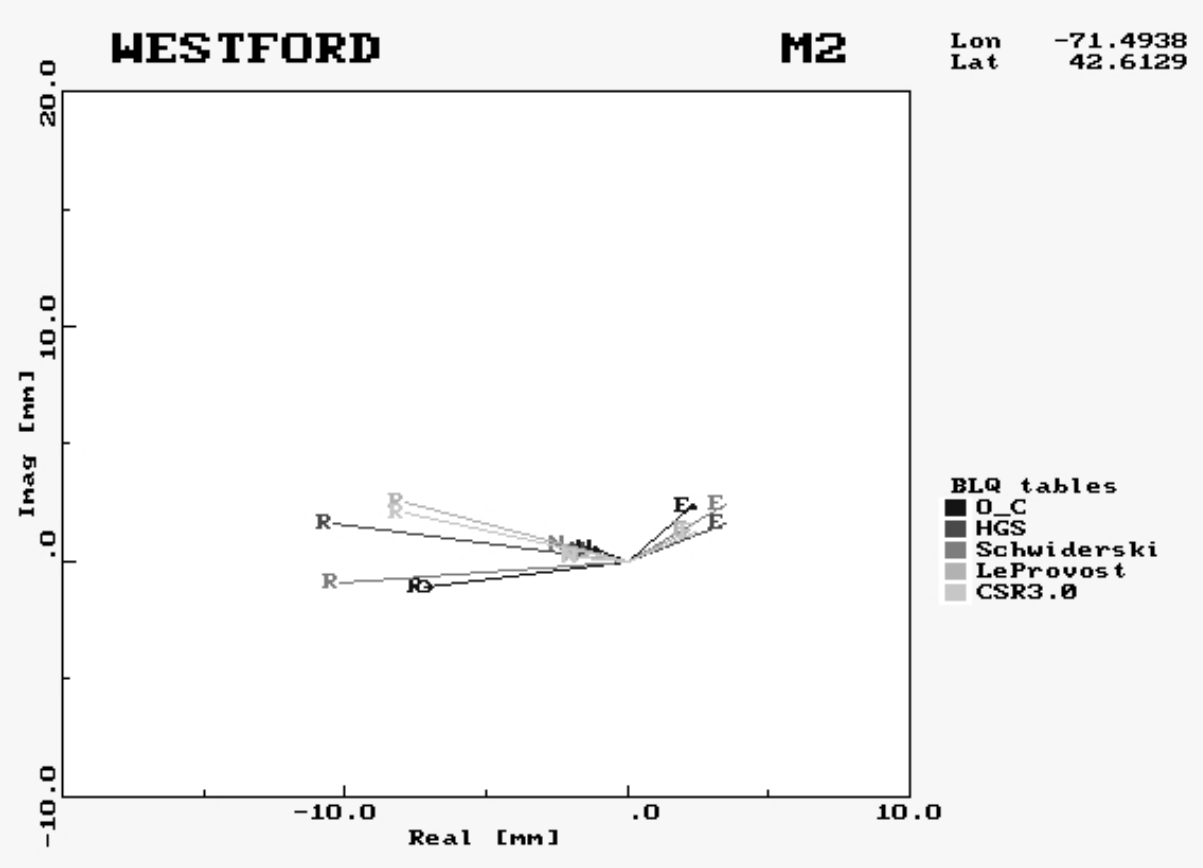

Figure 1: M_2 tide at Westford, Massachusetts. Observed motion in VLBI is indicated by light grey arrows with 95% confidence circle. Components Radial (=vertical), North and East are indicated by the capital letters. Ocean loading models are coded by grey-scale, see the legend.

a few cases less good agreement with the others; the Grenoble model (Le Provost et al., 1994) CSR3.0 (Eanes and Bettadpur, 1995), have not modelled the Bay of Fundy. The model labelled HGS is along the lines of Scherneck (1991a) and augments the Grenoble model in the missing area. It is generally found that Schwiderski's models compete quite well with more recent ones when loading on the shelves is considered. This is probably the effect of using a large number of coastal tide gauges, from which there is a great amount of high-quality data available particularly in the Atlantic area. In Fig. 2 a more abridged plot of the situation at three VLBI stations is shown. The diagrams shows all spatial components separately; the M_2 and O_1 tides have been combined (root square sum), first the observed effect and subsequently the residual when each model is applied.

GPS results are compiled in Tab. 2 for a comparison of loading due to the NSWC model (Naval Surface Weapons Center, Schwiderski and Szeto, 1982), the CSR3.0 model (Eanes and Bettadpur, 1995), and two model versions where we have added the centre of mass tide, denoting them CSR3.0-CMC and CSR3.1-CMC. The latter model has been adjusted to produce the centre of mass terms as reported in Watkins and Eanes (1997).

The test for the admittance of centre of mass tide into GPS is most sensitive at stations located far inland. One suitable site is Irkoutsk in Siberia. In Fig. 4 we show the model misfit at three locations (Irkoutsk, Ascension Island, Pie Town), and Fig. 3 details the situation for the M_2 tide at Irkoutsk. As suspected, the centre of mass components are not visible in the GPS data. We have investigated ten stations altogether (Reykjavik, Mauna Kea, Ascension Island, Onsala; Sundsvall, Yarragadee, Pie Town, Mendeleevo, Hartebeesthook) and found the results to point in the same direction, however less clear as crustal deformation components are regularly larger at coastal stations, particularly those in the first group.

More surprising with Irkoutsk is that the observed motion is close to the predicted motion although the signals are below one millimeter in amplitude. The error limit is based on the assumption of a phase

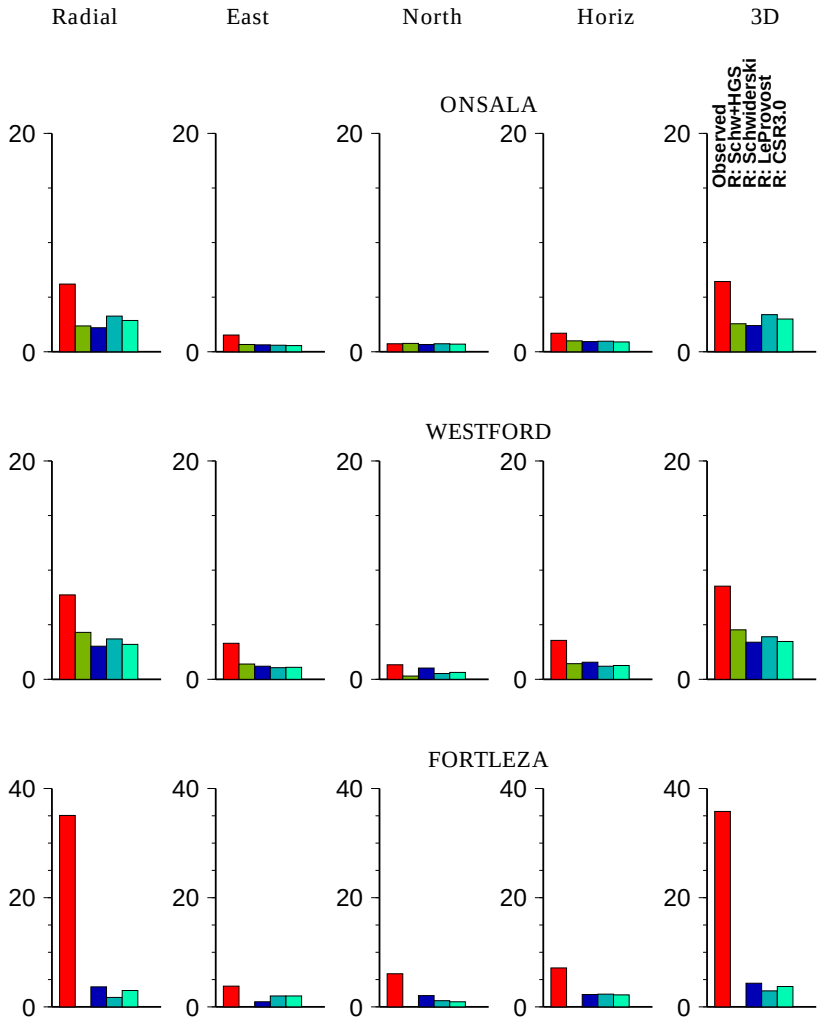

Figure 2: Modelling misfit for O_1 and M_2 tides at three VLBI stations. First column is radial (=vertical) direction, second east, third north, fourth horizontal (root square sum of east and north) and fifth the total root square sum. In each frame the first bar shows the observed effect and the other bars the residual effect (observed minus model, always vectorial amplitudes).

measurement accuracy of 10 cm and from that front-end assumption carried through the analysis. For more details, especially the accuracy of the satellite clock parameter that is crucial in single point positioning refer to Zumberge et al. (1997). The tidal post-fit normalized residual χ^2 is only slightly greater than unity in the vertical component and less than unity in the horizontal components, which hints at a resolution capability of subdiurnal motion of much less than a millimeter from two years of GPS. The method of interleaving of data batches over the day boundary, however, requires reformulation in order to avoid the biases we are seeing at solar synchronous cycles. They are not supposed to leak into the lunar frequencies, though, since the total length of the data assertains frequency selectivity narrower than one cycle per year, while only two cycles per month are required here.

Conclusions

We could show that ocean loading effects are observable with VLBI and GPS. We have restricted our scan to lunar species as these are largely unaffected by environmental perturbations and spurious effects due to earth rotation variations and satellite orbits. In VLBI the detectability of horizontal components due to ocean loading tides mark new, previously unreported results. In GPS the level of noise is greater, and horizontal motion is only marginally significant. As the vertical components of tide loading is

Table 1: Ocean loading at VLBI stations. Results show combined (root square sum) lunar effects at the diurnal period of O_1 and the semidurnal M_2. Lines marked R show vertical component, H horizontal. Values are in mm. Uncertainty σ is specified for M_2; for O_1 the uncertainty is about 30 percent greater. All cases show significant reduction of effect in all spatial components. Loading effects are computed from the models of NSWC - Schwiderski and Szeto (1982), Grenoble - Le Provost et al. (1994), and CSR3.0 - Eanes and Bettadpur (1995).

Site	C	σ	Observed	——— Residuals ———		
				NSWC	Grenoble	CSR3.0
FORTLEZA	R	0.7	35.1	3.7	1.8	3.0
	H	0.3	7.1	2.3	2.3	2.2
GILCREEK	R	0.3	9.7	1.5	1.2	0.8
	H	0.1	3.2	0.8	1.0	0.9
HARTEBEE	R	0.9	17.3	3.6	3.0	3.1
	H	0.5	2.9	2.2	1.8	2.0
KOKEE	R	0.4	13.7	3.4	3.4	2.3
	H	0.2	5.0	0.8	0.7	0.7
MOJAVE12	R	0.5	7.3	2.2	2.0	2.1
	H	0.2	4.2	1.5	0.6	0.7
ONSALA60	R	0.4	6.2	2.2	3.3	2.9
	H	0.2	1.7	0.9	1.0	0.9
RICHMOND	R	0.5	7.1	2.1	3.4	1.9
	H	0.2	4.2	0.8	0.8	0.9
WESTFORD	R	0.2	7.7	3.0	3.7	3.2
	H	0.1	3.6	1.6	1.2	1.3
WETTZELL	R	0.2	5.4	0.9	1.3	1.0
	H	0.1	1.9	1.3	1.1	1.0

regularly larger than a few millimeters, this component can be resolved with a better signal to noise ratio.

It appears most clear that differential frame motion between the stations and the satellite orbits is not affected by the centre of mass tide. This is probably a consequence of the treatment of the tracking stations in the orbit analysis where this effect is ignored, while the contribution from deformation at these stations is corrected for.

References

Dziewonski, A. and Anderson, D.L., 1981. Preliminary reference earth model, *Phys. Earth Planet. Int.,* **25,** 297–356.

Eanes R.J. and Bettadpur S., 1995: The CSR 3.0 global ocean tide model, *Technical Memorandum CSR-TM-95-06,* Center for Space Research, University of Texas, Austin, Tx.

Farrell, W.E., 1972. Deformation of the earth by surface loads, *Rev. Geophys. Space Phys.,* **10,** 761-797.

Haas, R., 1996. *Untersuchungen zu Erddeformationsmodellen für die Auswertung von geodätischen VLBI-Messungen*, PhD-thesis, Deutsche Geodätische Kommission, Reihe C, Heft Nr. 466, 103 pp.

Table 2: Ocean loading at GPS stations. Results show combined (root square sum) lunar effects at the diurnal periods of O_1 and Q_1 and the semidurnal M_2 and N_2. See caption of Tab. 1 for notations. Two versions of centre of mass tides are accounted for (label -CMC, CSR3.1-CMC being due to Watkins and Eanes, 1997). Error values apply to detection of a semidurnal oscillation.

Site	C	σ	Observed	Residuals			
				NSWC	CSR3.0	CSR3.0 -CMC	CSR3.1 -CMC
Reykjavik	R	0.9	18.9	5.5	5.4	6.0	8.1
	H	0.6	5.2	2.6	2.6	4.7	8.1
Sundsvall	R	0.8	2.9	2.1	1.7	3.5	5.6
	H	0.6	2.3	2.3	2.2	3.5	7.7
Pietown	R	1.0	4.8	1.7	0.9	2.9	5.1
	H	0.8	2.8	1.7	1.8	3.9	7.4
Hartebeesthoek	R	2.2	15.7	11.6	10.7	9.0	10.3
	H	2.0	4.9	4.8	5.0	5.9	7.5
Irkoutsk	R	0.9	1.6	2.0	1.9	2.2	3.3
	H	0.7	1.4	1.9	2.0	4.9	9.4
Ascension Isl.	R	1.4	12.8	10.4	11.9	10.2	11.2
	H	1.2	2.5	5.4	4.9	7.1	10.0
Yarragadee	R	1.2	6.8	13.3	13.3	13.7	13.7
	H	1.0	3.1	3.7	3.8	6.3	9.8
Mauna Kea	R	1.2	13.7	3.3	5.5	7.1	9.8
	H	1.0	4.7	2.2	2.7	5.1	7.5
Mendeleevo	R	1.0	2.1	1.4	1.6	3.1	5.5
	H	0.7	1.5	1.4	1.2	3.9	7.7
Onsala	R	0.7	5.1	1.7	2.0	3.7	6.6
	H	0.5	13.1	12.3	12.4	12.4	14.7

Haas, R. and Schuh, H., 1998. Ocean loading observed by geodetic VLBI, in Ducarme, B. (ed.), *Proc. 13'th Int. Symp. Earth Tides Brussels 1996*, in print.

Le Provost, C., Genco, M. L., Lyard, F., Vincent, P., and Canceil, P., 1994: Spectroscopy of the world ocean tides from a finite element hydrological model, *J. Geophys. Res.*, **99**, 24777–24798.

McCarthy, D. D. (ed): *IERS Conventions* IERS Technical Notes 21, Observatoire de Paris, 94 pp. 1996, and `http://hpiers.obspm.fr/webiers/general/syframes/convent/CONV.html`

Scherneck, H.-G., 1991. A parametrized solid earth tide model and ocean tide loading effects for global geodetic baseline measurements, *Geophys. J. Int.,* **106,** 677–694.

Scherneck, H.-G., 1991a. Regional ocean tide modelling, in *Proc. Eleventh Int. Symp. Earth Tides,* pp. 345-354, ed. Kakkuri, J., Schweizerbart, Stuttgart.

Scherneck, H.-G., and Webb, F.H., 1998. Ocean tide loading and diurnal tidal motion of the solid earth centre, *IERS(1998) Technical Note No 25.*, Observatoire de Paris, in print.

Schuh, H. and Haas, R., 1998. Earth tides in VLBI observations, in Ducarme, B. (ed.), *Proc. 13'th Int. Symp. Earth Tides Brussels 1996*, in print.

Schwiderski E. W. and Szeto, L. T., 1981, The NSWC global ocean tide data tape (GOTD), its features and application, random-point tide program, *NSWC-TR 81-254,* Naval Sur-

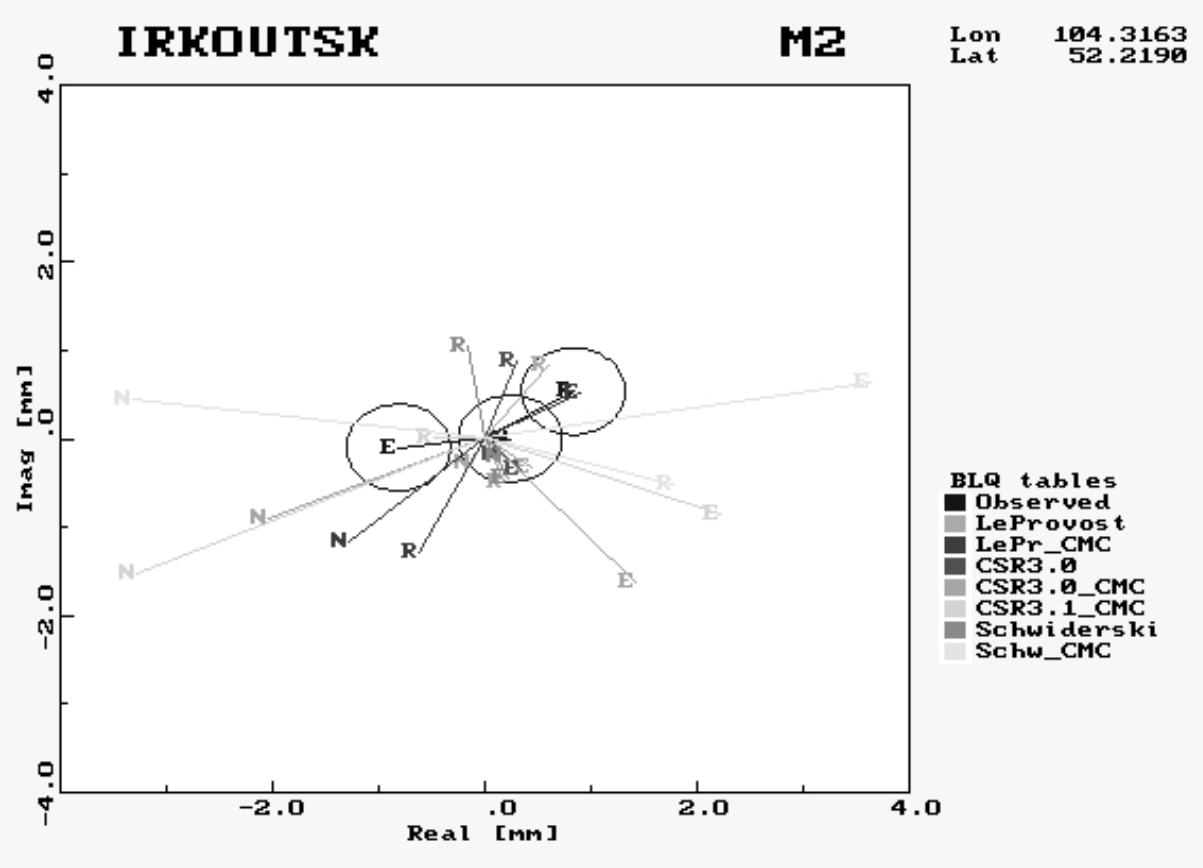

Figure 3: Like Fig. 1, but GPS at Irkoutsk, Siberia. This is an extreme inland station, which therefore is prone to exhibit global frame related motion. The loading models that incorporate frame translations are labelled _CMC and shown in light greys. They predict much larger motion than what is oberved.

face Weapons Center, Dahlgren Va., 19 pp.

Sovers, O. J., 1994. Vertical ocean loading amplitudes from VLBI measurements, *Geophys. Res. Letters,* **21,** 357–360.

Watkins M.M. and Eanes R.J., 1997: Observations of tidally coherent diurnal and semidiurnal variations in the geocenter, *Geophys. Res. Letters,* **24**, 2231–2234.

Webb F H, Zumberge J F, 1993: An Introduction to GIPSY/OASIS-II Precision Software for the Analysis of Data from the Global Positioning System, *JPL Publ. No. D-11088,* Jet Propulsion Laboratory, Pasadena, Cal.

Zumberge J F, Heflin M B, Jefferson D C, Watkins M M, Webb F H, 1997: Precise point positioning for the efficient and robust analysis of GPS data from large networks. *J. Geophys. Res.,* **102**, 5005–5017.

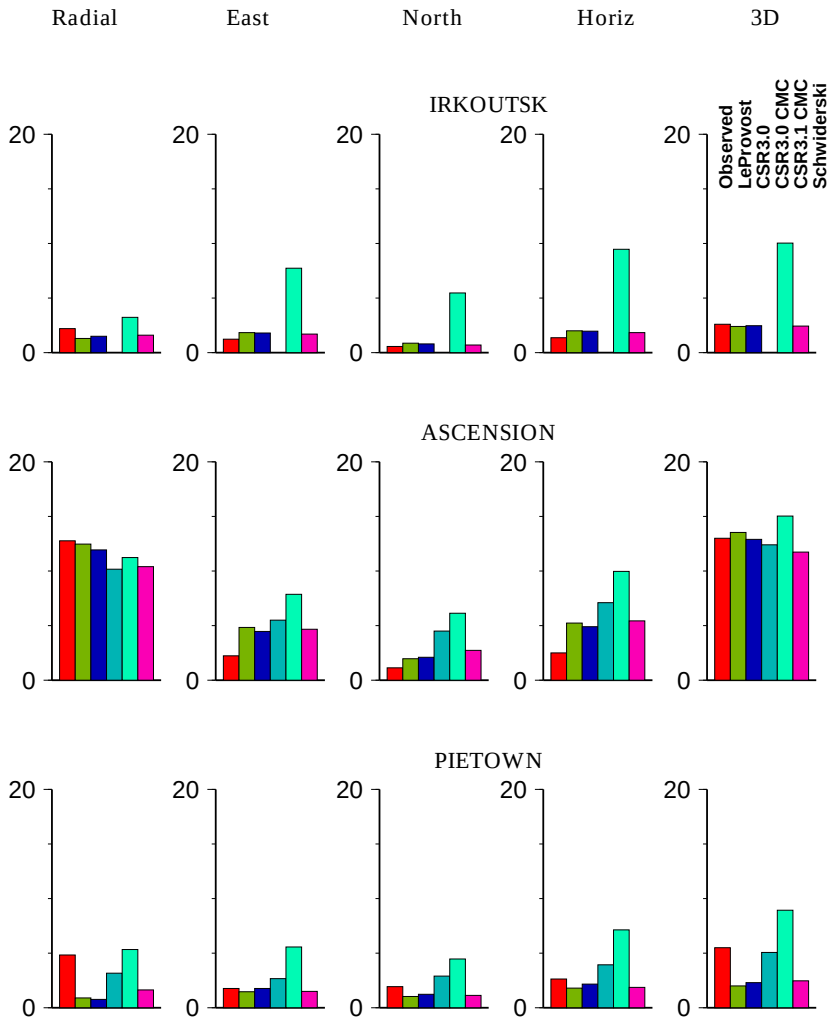

Figure 4: Like Fig. 2, but for GPS. Model and misfits consider four lunar tides, O_1, Q_1, N_2 and M_2. A general tendency is difficult to extract from this figure alone. Where residuals are low, the largest misfit occurs with the use of centre of mass tides. This seems to indicate that the GPS satellite orbit data is affected by the earth-fixed frame translations (as the tracking stations are not corrected for this motion), and thus the range to user stations is unaffected. The motion due to deformation, however, is visible since it is regularly modelled at the GPS orbit analysis stage, and it is geographically variable.